CHAPTER SIX

Flexible Membrane Inclusions and Membrane Inclusions Induced by Rigid Globular Proteins

Miha Fošnarič,[1] Aleš Iglič,[1] Tomaž Slivnik,[1] *and* Veronika Kralj-Iglič[2,*]

Contents

Abstract

We present a theoretical approach to the study of flexible membrane inclusions and membrane inclusions induced by rigid membrane-embedded proteins. We derive the contribution to the free energy of the membrane bilayer for both kinds of inclusions. For flexible membrane inclusions, the phenomenological interaction constants that appear in the free energy expression depend on the physical and geometrical properties of the molecules that constitute the inclusion. The cases of constrained and unconstrained local shape perturbations of the membrane around a rigid membrane inclusion are discussed. The total free energy of membrane bilayer with membrane-embedded inclusions (membrane nanodomains) is derived.

* Corresponding author. Tel.: +386 41 720766; Fax: +386 1 4768850;
E-mail address: veronika.kralj-iglic@fe.uni-lj.si (V. Kralj-Iglic).

[1] Laboratory of Physics, Faculty of Electrical Engineering, University of Ljubljana, Tržaška 25, SI-1000 Ljubljana, Slovenia
[2] Laboratory of Clinical Biophysics, Faculty of Medicine, University of Ljubljana, Lipičeva 2, SI-1000 Ljubljana, Slovenia

Advances in Planar Lipid Bilayers and Liposomes, Volume 7
ISSN 1554-4516, DOI: 10.1016/S1554-4516(08)00006-9

1. Introduction

Membrane inclusions are important functional building blocks of biological membranes. As an addition to the lipid bilayer(s), they can significantly increase the complexity and alter the physical properties of biological membranes.

In this work, we divide membrane inclusions into two groups. In the first are *flexible membrane inclusions*, which are small complexes composed of proteins and lipids where the proteins are often chain-like biopolymers that cross the membrane bilayer a few times (Fig. 1A) [1]. Membrane nanodomains and raft elements of biological membranes usually fall into this category. The second group are membrane inclusions (membrane nanodomains) induced by a *single rigid globular membrane protein*, which can be described in the first approximation as a rigid object of a simple geometrical shape (Fig. 1B) [2]. Some of the membrane-embedded peptides may induce such inclusions (nanodomains). The scope of this contribution is to derive a single-inclusion energy for both kinds of biological inclusions (i.e., membrane nanodomains).

2. Flexible Anisotropic Membrane Inclusions

Thin surface of the membrane is in general anisotropic with respect to the curvature of the normal cuts [3–5] and can attain various equilibrium shapes that are not flat or spherical [6].

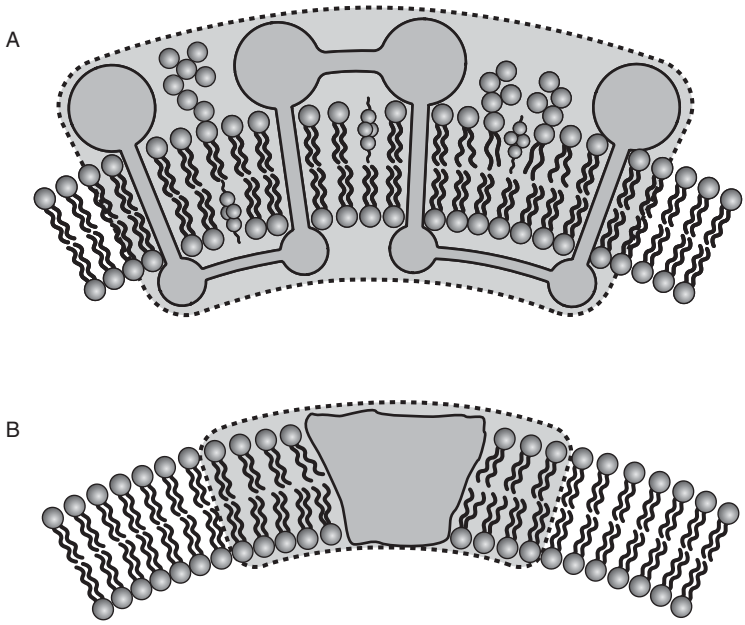

Figure 1 Schematic illustration of membrane inclusions (shaded area): a flexible membrane inclusion (A) and a membrane inclusion induced by membrane-embedded rigid protein (B).

The local shape of the membrane surface is described by two principal curvatures C_1 and C_2 (Fig. 7). The flexible membrane inclusion is treated as a small two-dimensional flexible plate with area a_0. The inclusion is in general anisotropic; therefore, its intrinsic shape can be described by the two intrinsic principal curvatures, C_{1m} and C_{2m} (Fig. 2) and by the in-plane orientation of the inclusion in the membrane (Fig. 3).

Accordingly, we define the elastic energy of a small plate-like membrane inclusion (1) with area a_0 as the energy of the mismatch between the actual local curvature of the membrane and the intrinsic (spontaneous) curvature of the inclusion. Therefore, we define the tensor [5] $\underline{M} = \underline{R}\,\underline{C}_m\,\underline{R}^{-1} - \underline{C}$, where the tensor $\underline{C}$ describes the actual local curvature, the tensor $\underline{C}_m$ describes the intrinsic curvature of the protein (Fig. 2), and

$$\underline{R} = \begin{bmatrix} \cos\omega & -\sin\omega \\ \sin\omega & \cos\omega \end{bmatrix} \tag{1}$$

is the rotation matrix (see also Fig. 3). In the respective principal systems, the matrices that represent curvature tensors include only the diagonal elements:

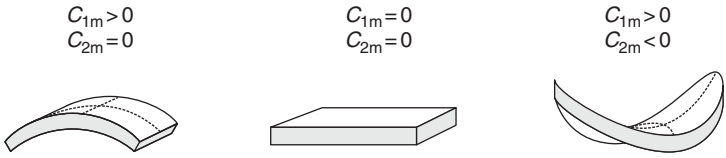

Figure 2 Schematic illustration of the most favorable shapes of flexible membrane inclusions having different values of their intrinsic (spontaneous) curvatures C_{1m} and C_{2m}.

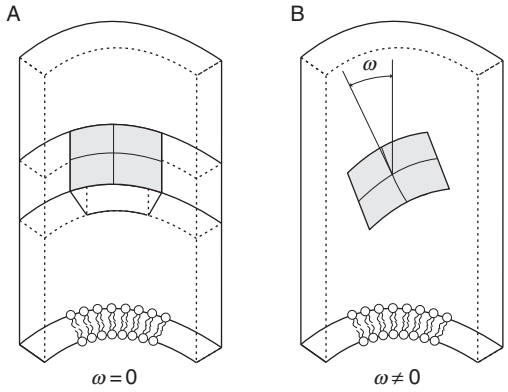

Figure 3 Schematic illustration of different orientations of a flexible membrane inclusion with intrinsic principal curvatures $C_{1m} > 0$ and $C_{2m} = 0$ (see also Fig. 2). The shape of the membrane is cylindrical ($C_1 > 0$ and $C_2 = 0$).

$$\underline{C} = \begin{bmatrix} C_1 & 0 \\ 0 & C_2 \end{bmatrix}, \quad \underline{C}_{\mathrm{m}} = \begin{bmatrix} C_{1\mathrm{m}} & 0 \\ 0 & C_{2\mathrm{m}} \end{bmatrix}. \tag{2}$$

The principal systems of these two tensors are in general rotated in the tangent plane of the membrane surface by an angle ω with respect to each other (Fig. 3).

The elastic energy of the inclusion per unit area (w) should be a scalar quantity. Therefore, each term in the expression for w must also be a scalar [7], that is, invariant with respect to all transformations of the local coordinate system. In this work, the elastic energy density w is approximated by an expansion in powers of all independent invariants of the tensor $\underline{M}$ up to the second order in the components of $\underline{M}$. The trace and the determinant of the tensor are taken as the set of invariants [5, 8]:

$$w = \mu_0 + \frac{K_1}{2}(\mathrm{Tr}\,\underline{M})^2 + K_2 \mathrm{Det}\,\underline{M}, \tag{3}$$

where μ_0 is the minimal possible value of w, while K_1 and K_2 are constants. For the sake of simplicity, $\mu_0 \equiv 0$. Taking into account the definition of the tensor $\underline{M}$, it follows from Eqs. (2) and (3) that the elastic energy of the flexible membrane inclusion can be written as:

$$E = a_0(2K_1 + K_2)(H - H_{\mathrm{m}})^2 - a_0 K_2 (D^2 - 2DD_{\mathrm{m}}\cos 2\omega + D_{\mathrm{m}}^2), \tag{4}$$

where

$$H = \frac{1}{2}(C_1 + C_2), \tag{5}$$

is the membrane mean curvature,

$$D = \frac{1}{2}|C_1 - C_2|, \tag{6}$$

is the membrane curvature deviator, $H_{\mathrm{m}} = (C_{1\mathrm{m}} + C_{2\mathrm{m}})/2$ is the intrinsic (spontaneous) mean curvature, and $D_{\mathrm{m}} = |C_{1\mathrm{m}} - C_{2\mathrm{m}}|/2$ is the intrinsic (spontaneous) curvature deviator.

It can be seen from Eq. (4) that the material properties of an anisotropic flexible membrane inclusion can be expressed in a simple way by only two intrinsic curvatures $C_{1\mathrm{m}}$ and $C_{2\mathrm{m}}$ and constants K_1 and K_2. Figure 2 shows a scheme of a cylindrical, flat, and saddle-like intrinsic (spontaneous) shapes of the flexible membrane inclusions.

The values of the membrane mean curvature $H = (C_1 + C_2)/2$, the curvature deviator $D = |C_1 - C_2|/2$, and the orientation angle of the inclusion ω that correspond to the minimum of the function E for given values of $H_{\mathrm{m}} = (C_{1\mathrm{m}} + C_{2\mathrm{m}})/2$

and $D_m = |C_{1m} - C_{2m}|/2$, can be calculated from the necessary conditions for the extremum of the function E [8]:

$$\frac{\partial E}{\partial H} = 2a_0(2K_1 + K_2)(H - H_m) = 0, \tag{7}$$

$$\frac{\partial E}{\partial D} = -K_2 a_0(2D - 2D_m \cos 2\omega) = 0, \tag{8}$$

$$\frac{\partial E}{\partial \omega} = -4a_0 K_2 D D_m \sin 2\omega = 0, \tag{9}$$

and the sufficient conditions for the minimum of E [9]:

$$\frac{\partial^2 E}{\partial H^2} = 2a_0(2K_1 + K_2) > 0, \tag{10}$$

$$\left(\frac{\partial^2 E}{\partial H^2}\right)\left(\frac{\partial^2 E}{\partial D^2}\right) - \left(\frac{\partial^2 E}{\partial H \partial D}\right)^2 = -4K_2 a_0^2(2K_1 + K_2) > 0, \tag{11}$$

$$\begin{aligned} &\frac{\partial^2 E}{\partial H^2}\left[\left(\frac{\partial^2 E}{\partial D^2}\right)\left(\frac{\partial^2 E}{\partial \omega^2}\right) - \left(\frac{\partial^2 E}{\partial D \partial \omega}\right)^2\right] \\ &= 16K_2^2 a_0^3 \frac{\partial^2 E}{\partial H^2}(D D_m \cos 2\omega - D_m^2 \sin^2 2\omega) > 0, \end{aligned} \tag{12}$$

where it was taken into account that $\partial^2 E/\partial H \partial D = 0$ and $\partial^2 E/\partial H \partial \omega = 0$. Considering only positive values of ω, it follows from Eqs. (7) to (9) and (12) that at the minima of E:

$$H = H_m, \quad D = D_m, \quad \omega = 0, \pi, \tag{13}$$

and [8]

$$K_1 > -K_2/2, \quad K_2 < 0. \tag{14}$$

If flexible membrane inclusions have $C_{1m} > 0$ and $C_{2m} = 0$ (see Fig. 2), the energetically favorable membrane shapes would be tubular or collapsed tubular (in the form of a twisted strip—helix A, see Fig. 4). For $C_{1m} > 0$ and $C_{2m} < 0$ (see Fig. 2), the favorable membrane shape would be saddle like (constituting the neck connecting the daughter vesicle and the parent cell) or the collapsed tubular, twisted in the form of a helix B strip (see Fig. 4 and [5]).

The flexible membrane inclusion adapts its shape in order to fit its curvature to the actual membrane curvature (which is also influenced by inclusions). Since all

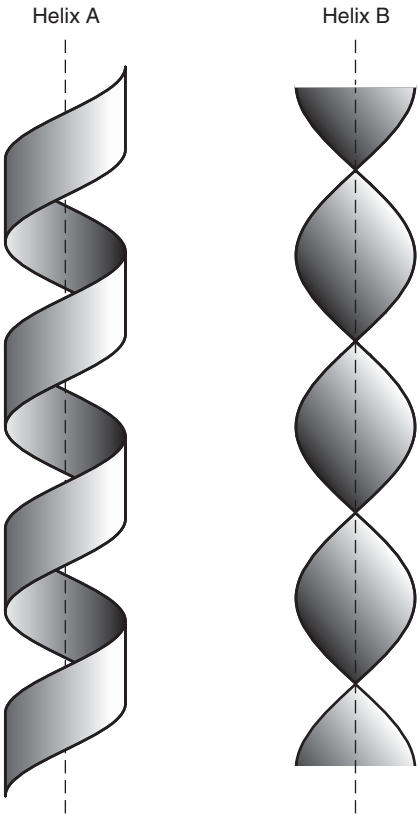

Figure 4 Schematic presentation of a helical (A and B) configuration.

orientations of the single flexible inclusion do not have the same energy [see Eq. (4)], the partition function of a single inclusion can be written in the form:

$$Q = \frac{1}{\omega_0}\int_0^{2\pi} \exp\left(-\frac{E(\omega)}{kT}\right) \mathrm{d}\omega, \tag{15}$$

with ω_0 as an arbitrary angle quantum. The free energy of the flexible membrane inclusion is then obtained by the expression $f_i = -kT\ \ln Q$. Combining Eqs. (4) and (15) allows us to write the free energy of a single flexible membrane inclusion up to the constant as:

$$\begin{aligned} f_i = {} & (2K_1 + K_2)(H - H_\mathrm{m})^2 a_0 - K_2(D^2 + D_\mathrm{m}^2)a_0 \\ & -kT\ \ln\left(I_0\left(\frac{2K_2 D D_\mathrm{m} a_0}{kT}\right)\right). \end{aligned} \tag{16}$$

By knowing the equilibrium density distribution of the membrane inclusions over the membrane [10], the contribution of the inclusions to the overall membrane's free energy can be attained by integration of Eq. (16) over the whole membrane surface. This possibility makes the above described approach an efficient theoretical tool to study equilibrium (closed) shapes of membranes with (in general anisotropic) membrane inclusions [11–13].

3. Membrane Inclusions Induced by the Rigid Membrane-Embedded Protein

3.1. Perturbation of Lipid Molecules Around Rigid Membrane-Embedded Proteins

A rigid protein, intercalated in the lipid bilayer, perturbs the structure of the surrounding lipids. Therefore, we can define the membrane inclusion as the embedded rigid protein and the surrounding lipids that are significantly distorted due to the presence of the embedded rigid protein [11]. The energy of such membrane inclusion induced by an embedded rigid protein is therefore mainly attributed to the change of the energy of the surrounding lipids. The energy of lipid molecule depends on the particular sequence of *trans*, *gauche*$^+$, and *gauche*$^-$ orientations along the lipid chain, the van der Waals interactions of lipid chain with its neighbors, steric repulsion between hard cores of each atom of neighboring lipid chains, and ionic interactions between polar lipid headgroups [14, 15]. The change in the ordering of lipids that surround the rigid protein leads to an indirect lipid-mediated interaction between two rigid proteins when they approach each other [15]. If the two proteins are close enough, the total lipid perturbation decreases, which may result in a net attractive force between the membrane-embedded rigid proteins and therefore in their aggregation [15].

Cone-like rigid proteins [2] are characterized by a cone-angle onto which the membrane shape has to adapt. The mesoscopic-level description of the membrane identifies the rigid protein's cone-shape with a local discontinuity in the membrane curvature field. On a more microscopic level, another degree of freedom of the membrane becomes significant, namely the *tilt* of the lipid molecules [16, 17]. Helfrich and Prost [3] have shown that symmetric lipid bilayer may exhibit an intrinsic bending force if the lipid molecules are collectively tilted.

However, membrane perturbations that involve lipid tilt are often short-ranged, with a characteristic length extending over a few lipids. Lipid tilt is thus important for processes where the local membrane geometry changes over short distances such as for non-bilayer lipid phases [18, 19], or for the periodic "ripple" phase [20–22].

In the theoretical works cited above, the membrane-embedded rigid proteins exhibit cylindrical symmetry about their axis normal to the membrane, that is, they are *isotropic*. More general, if cylindrical symmetry of rigid membrane protein is absent (Fig. 5), the membrane inclusion free energy depends on the protein's in-plane orientation within the membrane. The intrinsic shape of the rigid protein is then characterized by two intrinsic principal curvatures, C_{1m} and C_{2m}. The lateral

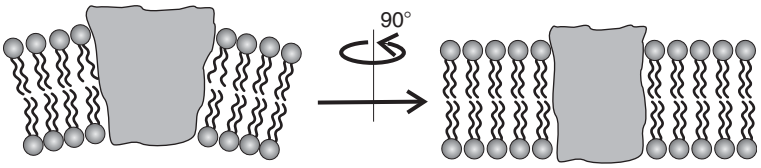

Figure 5 Schematic illustration of an *anisotropic* membrane-embedded rigid protein.

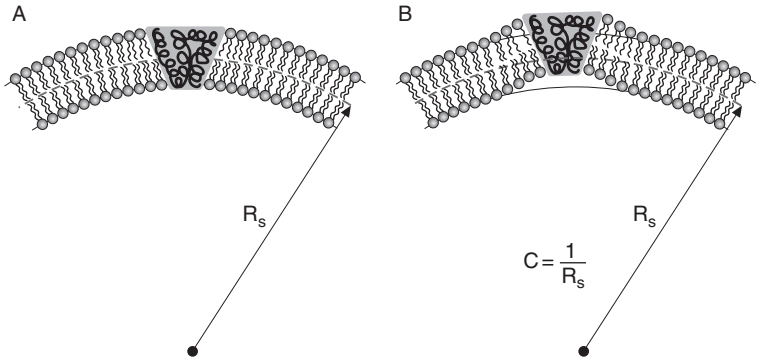

Figure 6 Schematic illustration of the lipid bilayer of prescribed spherical curvature $(C = C_1 = C_2 = H = 1/R_s)$ defined at mesoscopic scale level. The intercalated rigid protein has conical shape. In the case A the local membrane shape does not differ from the mesoscopic spherical curvature of the membrane (c), while in the case B also the local microscopic (nano-scale) membrane shape perturbation of the spherical surface with curvature c is induced due to the presence of the rigid protein. In the case B lipids accommodate to the intrinsic shape of the intercalated rigid protein through the curvature deformation and via changes in lipid tilt, while in the case A lipids accommodate to the protein intrinsic shape via changes in lipid tilt (adapted from [28]).

organization of *anisotropic* proteins can be quite complex, ranging from chain-like assembly [23], saddle-like membrane regions [11] to periodic pattern formation [24].

Within the standard theory of elasticity of lipid bilayer, its elastic energy is decomposed into contributions due to area stretching, tilt of the lipid molecules, local bending, and non-local bending [16, 25, 26]. On a mesoscopic-scale level, the local and non-local bending energies can be described in terms of its two local principal membrane curvatures C_1 and C_2 [25, 26]. The question arises, how the elastic behavior of a membrane bilayer is affected by membrane-embedded rigid proteins, if the local microscopic membrane shape perturbation (at the nano-scale level) due to each individual protein is taken into account (Fig. 6). In general, the theoretical description of local microscopic perturbations of lipid molecules around the intercalated rigid protein falls in between the two limiting cases.

In the first case, the membrane intercalated rigid proteins are distributed over the whole membrane surface or at least over a large portion of it (see also [1]). Therefore, possible local microscopic perturbations of the membrane shape around each of the rigid proteins (as schematically shown in Fig. 6B) would greatly increase the non-local bending energy of the bilayer membrane. This energy contribution, also called

the relative stretching energy (since it originates from different stretching of both monolayers during bending of the bilayer at constant average membrane area) [25–27], can be written as

$$W_{\mathrm{n}} = k_{\mathrm{n}} A(\langle H\rangle - H_0)^2, \tag{17}$$

where $\langle H\rangle = \frac{1}{A}\int H\mathrm{d}A$ is the average mean curvature, $H = (C_1 + C_2)/2$, H_0 is the spontaneous mean curvature [12], k_{n} is the non-local bending rigidity [27], A is the membrane area, and $\mathrm{d}A$ is the membrane area element. For a closed, nearly flat bilayer membrane (where $\langle H\rangle \approx 0,\ H_0 \approx 0$), with N homogeneously distributed intercalated rigid proteins, the membrane's non-local bending energy W_{n} can be approximately written as [28]

$$W_{\mathrm{n}} \cong k_{\mathrm{n}} A(N\langle H\rangle_{\mathrm{p}} - NH_{0\mathrm{p}})^2 \propto N^2, \tag{18}$$

where $H_{0\mathrm{p}}$ and $\langle H\rangle_{\mathrm{p}}$ refer to the disturbed membrane patch around single membrane-intercalated rigid protein (Fig. 6B). Since the energy W_{n} increases quadratically with the total number of membrane-embedded rigid proteins, the local microscopic perturbation of the membrane shape around each of the intercalated rigid proteins (Fig. 6B) would be energetically less favorable for large enough N than the locally unperturbed membrane shape where the lipids accommodate to intrinsic shape of rigid protein predominantly via changes in the lipid tilt (Fig. 6A).

In the opposite limit, the membrane region with intercalated rigid proteins is spatially confined (i.e., small) and in contact with a reservoir of relaxed lipid bilayer. Therefore, the lipids surrounding the intercalated rigid protein are free to adjust their conformation also by perturbation of the local membrane shape, as schematically shown in Fig. 6B.

In biological membranes, the majority of the membrane proteins are laterally distributed over the whole membrane area. In addition, the number of the membrane proteins (N) is very large. Therefore, the first scenario, that is, the case of constrained microscopic deviations of the membrane shape around the intercalated rigid inclusions (Fig. 6A), seems to be more relevant [see also Eq. (18)].

3.2. Energy of Membrane Inclusion Induced by a Single Rigid Membrane Protein

Coupling between non-homogeneous lateral distribution of membrane-embedded rigid proteins and membrane shapes may be a general mechanism of generation and stabilization of highly curved membrane structures (spherical buds, membrane necks, thin tubular membrane protrusions) [11, 12, 29–32].

On the phenomenological level, membrane bending may couple energetically to the local density of membrane-embedded rigid proteins by introducing the composition-dependent local bending constant and spontaneous curvature. The underlying model (including also the direct interactions between rigid protein and

configurational entropy of rigid proteins) was suggested by Markin [29] and used in subsequent applications [33]. Leibler [34] proposed a similar thermodynamical model.

Another theoretical approach starts from a phenomenological expression for the energy of a *single* membrane inclusion induced by intercalation of the rigid protein [10, 11] where the term inclusion is used for an entity consisting of the embedded rigid protein and lipids that are significantly distorted due to the presence of the embedded rigid protein [11] (see also Fig. 1B).

It is proposed that the energy of such inclusion derives from the mismatch between the local shape of the membrane and the intrinsic shape of the membrane-embedded rigid protein. The local curvature of the membrane is represented by curvatures of all possible normal cuts of the surface through the site of the inserted rigid protein. The energy of a single inclusion induced by intercalation of single rigid protein is then given by a phenomenological expression consisting of two terms [11],

$$E = \frac{\xi}{4\pi}\int_0^{2\pi}(C - C_{\mathrm{m}})^2 \mathrm{d}\psi + \frac{\xi^*}{16\pi}\int_0^{2\pi}\left(\frac{\mathrm{d}}{\mathrm{d}\psi}(C - C_{\mathrm{m}})\right)^2 \mathrm{d}\psi, \qquad (19)$$

where ξ and ξ^* are positive interaction constants, C is the curvature of the membrane normal cut that is for an angle ψ rotated in the principal axes system of the membrane surface, C_{m} is the curvature of the normal cut corresponding to the protein intrinsic shape in the same direction. The first contribution takes into account the differences of the curvatures of the normal cuts of the two systems while the second contribution takes into account the coupling between the neighboring curvatures of the normal cuts of the two systems.

The orientation of the membrane-embedded rigid protein is described by considering that the principal directions of the membrane surface are in general different from the principal directions of the protein intrinsic shape. The mutual orientation of the two systems is determined by the angle ω. We consider the Euler equations for the curvatures of the respective normal cuts of the continuum

$$C = C_1 \cos^2\psi + C_2 \sin^2\psi \qquad (20)$$

and

$$C_{\mathrm{m}} = C_{1\mathrm{m}} \cos^2(\psi + \omega) + C_{2\mathrm{m}} \sin^2(\psi + \omega), \qquad (21)$$

where C_1 and C_2 are the principal curvatures describing the local shape of the surface (Fig. 7), and $C_{1\mathrm{m}}$ and $C_{2\mathrm{m}}$ are the principal curvatures describing the intrinsic shape of the membrane-embedded rigid protein.

By performing the integration in Eq. (19), we get

$$E = \mu_{\mathrm{m}} + \frac{\xi}{2}(H - H_{\mathrm{m}})^2 + \frac{\xi + \xi^*}{4}(D^2 - 2DD_{\mathrm{m}}\cos 2\omega + D_{\mathrm{m}}^2), \qquad (22)$$

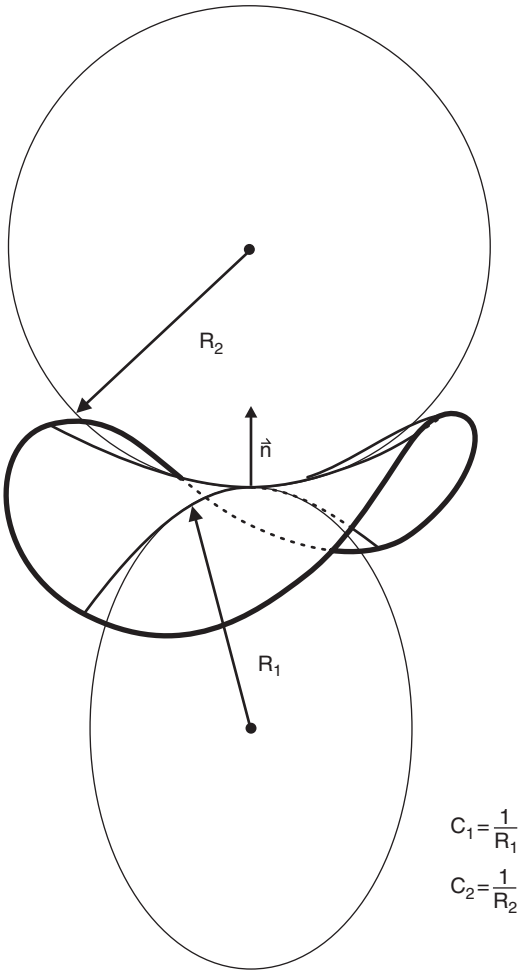

Figure 7 Schematic illustration of the two principal curvatures of membrane surface.

where μ_{m} is the constant, $H = (C_1 + C_2)/2$ is the mean curvature, $D = |C_1 - C_2|/2$ is the curvature deviator, while $H_{\mathrm{m}} = (C_{1\mathrm{m}} + C_{2\mathrm{m}})/2$ and $D_{\mathrm{m}} = |C_{1\mathrm{m}} - C_{2\mathrm{m}}|/2$ are the intrinsic mean and deviatoric curvatures that reflect the preferred local macroscopic membrane curvature of the membrane-embedded rigid protein. The membrane inserted protein is called isotropic if $C_{1\mathrm{m}} = C_{2\mathrm{m}}$, while it is called anisotropic if $C_{1\mathrm{m}} \neq C_{2\mathrm{m}}$. Figure 8 gives a schematic presentation of different intrinsic shapes of inserted rigid proteins.

At this point, let us stress that the energy of a single membrane inclusion induced by membrane-embedded rigid protein (Eq. 22) is mathematically equivalent to the energy of a single flexible membrane inclusion (Eq. 4). Combining both equations yields relations between the interaction constants, $\xi = 2a_0(2K_1 + K_2)$ and $\xi^* = -2a_0(2K_1 + 3K_2)$. However, the origin of the interaction constants can be

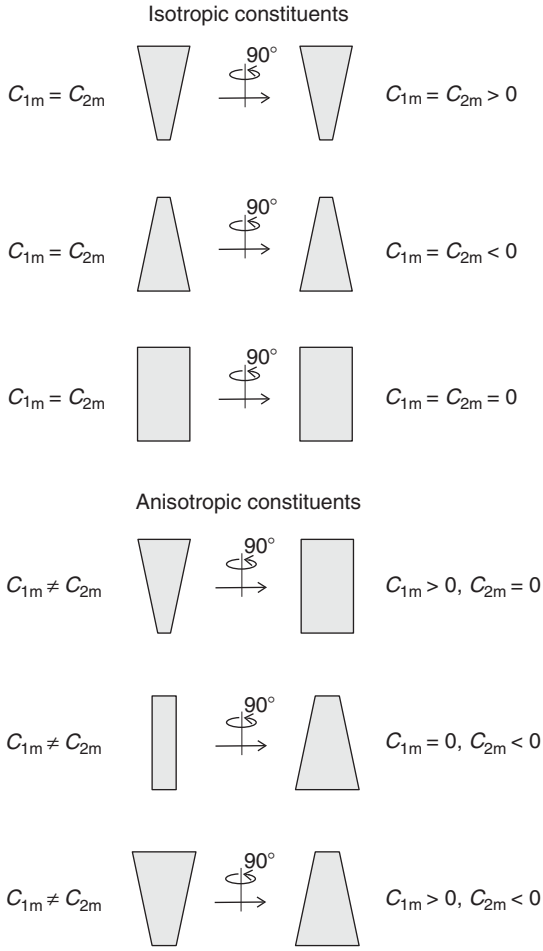

Figure 8 **Schematic illustration of different isotropic and anisotropic shapes of the membrane-embedded constituents (rigid proteins). The intrinsic shape of the protein is characterized by two intrinsic principal curvatures C_{1m} and C_{2m}.**

different in each case. Namely, in the case of a membrane inclusion induced by the membrane-embedded protein, the interaction constant originates in the deformation of the lipids surrounding the rigid protein, while in the case of a flexible membrane inclusion, the biopolymer(s) itself is (are) also deformed.

The maximum and the minimum of $E_i(\omega)$ are for protein orientation angle $\omega = 0$ and $\omega = \pi/2$, respectively. The single inclusion energy (Eq. 22) comprises the contribution due to deformation of the lipids that surround the intercalated protein (Fig. 6) [10, 11, 35].

The possible microscopic (nano-scale) perturbations of the membrane shape around the intercalated rigid protein (Fig. 6B) are not explicitly taken into account in Eq. (22), but rather hidden in the phenomenological constants μ_m, ξ, ξ^*, C_{1m}, and

C_{2m} (or H_m and D_m) (Fig. 8), where it is assumed that the distorted regions of lipids of the neighboring proteins do not overlap.

The concept of the single inclusion energy was taken as a base for a self-consistent description of equilibrium shapes of a closed bilayer vesicle and the related lateral distribution of intercalated inclusions [10, 11, 36]. In accordance with previous results [29], clustering and lateral phase separation of the inclusion has been predicted [1].

Within the above described phenomenological (mean-field) approach, the influence of membrane-embedded rigid proteins on the elastic properties of the lipid bilayer can be calculated in terms of the properties of the host membrane and the properties (geometry) of the intercalated rigid proteins. The non-homogeneous lateral distribution of the isotropic rigid proteins are an internal degree of freedom that lowers the equilibrium free energy of the membrane and in this way contributes to the decrease of the local bending modulus κ_c [10, 34, 36]. The change in the membrane elasticity depends linearly on the density of membrane-embedded rigid proteins. In the case of anisotropic rigid proteins, their rotational ordering is another internal degree of freedom, which additionally decreases the membrane local bending constant [11, 35].

4. Estimation of the Model Parameters

4.1. Basic Model

In the previous section, we derived the expression for the energy of the membrane inclusion (membrane nanodomain) induced by the membrane-embedded rigid protein. In this subsection, the phenomenological parameters describing the single inclusion energy H_m, D_m, and ξ [see Eq. (22)] are estimated using a simple theoretical model describing the elasticity of lipid bilayer [13].

In this analysis, we assume that the local microscopic shape deformations of the membrane around the membrane-embedded rigid protein are constrained (Fig. 6A) and the lipids accommodate to the intrinsic shape of rigid protein only via changes in the lipid tilt. This corresponds to the biologically relevant case of the membrane proteins that are distributed all over the cell membrane.

Let us consider a single cone-like rigid protein. To render the induced inclusion anisotropic, we introduce a dependency of the cone angle $\theta = \theta(\omega)$ on the azimuthal angle ω (Fig. 9). For small variations of θ, we can write

$$\theta(\omega) = \overline{\theta} + \Delta\theta \cos(2\omega), \tag{23}$$

where $\overline{\theta}$ is the average "cone-ness" of the protein and $\Delta\theta$ is the corresponding deviator.

The rigid protein is embedded in a lipid bilayer of mean and deviatoric curvatures H and D, respectively. Hence, according to the lemma of Euler, the curvature measured in the radial direction of the inclusion, at azimuthal angle ω, is

$$C(\omega) = H + D\cos(2\omega) \tag{24}$$

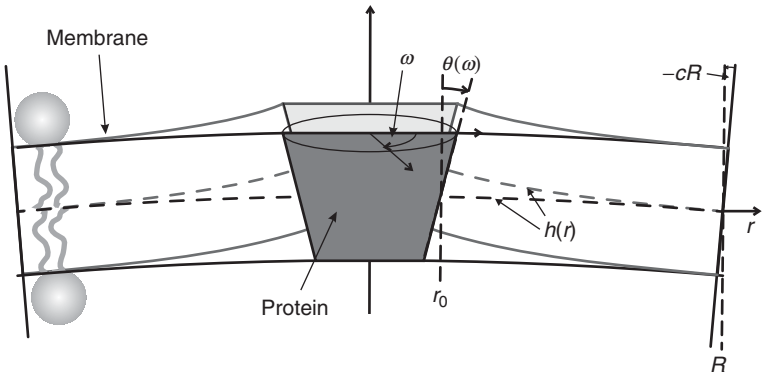

Figure 9 Schematic illustration of a protein in the membrane for the model of constrained (dark gray—in front) local shape perturbation from Section 5.2, and unconstrained (light gray—in back) local shape perturbations from Section 5.1. For anisotropic inclusions, the cone angle θ depends on the azimuthal angle ω.

Formally, the protein-induced perturbation free energy of the lipid bilayer can be expressed as an integration of the free energy density $\tilde{E}(\omega)$ per unit length of the circumference of the inclusion's core, $L = 2\pi r_0$, where r_0 is the radius of the inclusion's core (i.e., rigid protein): $E = \int_L \tilde{E} dL = (L/2\pi)\int \tilde{E}(\omega) d\omega$ (see Fig. 9). For sufficiently large radius r_0, we expect that $\tilde{E} = \tilde{E}[C(\omega), \theta(\omega)]$ depends only parametrically on ω, namely via the relations $C(\omega)$ and $\theta(\omega)$. More generally, $\tilde{E}$ should also depend on the derivatives of $C(\omega)$ and $\theta(\omega)$ with respect to ω. This additional dependence should become relevant if the radius r_0 were smaller than the characteristic decay length ζ of membrane perturbations. Using membrane elasticity theory, the characteristic decay length ζ has recently been calculated [37] for a planar ($C = 0$) lipid layer in contact with a wall tilted by an angle θ; it depends on the thickness of the lipid bilayer, the lateral stretching modulus, and the tilt modulus (κ_t). Typical values for a lipid monolayer [13] yield $\zeta = 0.9$ nm. Hence, assuming that $r_0 \geq \zeta$, we can write

$$\frac{E}{L} = \frac{1}{2\pi}\int_0^{2\pi} \tilde{E}[C(\omega), \theta(\omega)] \mathrm{d}\omega \tag{25}$$

In this case, $\tilde{E}$ can be calculated using a one-dimensional model for the elastic interaction of a lipid layer with an infinitely extensive, rigid wall. Such model has frequently been suggested in previous works [37, 38] and can be generalized to a bent lipid layer of curvature C [13],

$$\tilde{E}(C, \theta) = \frac{\kappa_0}{2\zeta}(\theta - Cr_0)^2 + (C_0 - C)(\theta - Cr_0), \tag{26}$$

where κ_0 is the bending stiffness of the lipid monolayer and C_0 is the spontaneous curvature.

After inserting $\theta(\omega)$ from Eq. (23) and $C(\omega)$ from Eq. (24) into Eq. (26), the comparison of the obtained expression with Eq. (22) yields [13]:

$$H_{\mathrm{m},1} = \frac{\overline{\theta}}{r_0}\left(\frac{r_0+\zeta}{r_0+2\zeta}\right) + \frac{\zeta C_0}{r_0+2\zeta}, D_{\mathrm{m},1} = \frac{\Delta\theta}{r_0}\left(\frac{r_0+\zeta}{r_0+2\zeta}\right) \tag{27}$$

$$\xi = 2\pi r_0^2 \kappa_0 \left(\frac{r_0}{\zeta}+2\right), \quad \xi^* = 0 \tag{28}$$

This confirms the expectation that the shape of the inclusion's core (i.e., the shape of membrane-embedded rigid protein) is incorporated in the expressions for the spontaneous mean curvature and the spontaneous curvature deviator so that $H_{\mathrm{m},1} = \overline{\theta}/r_0$ and $D_{\mathrm{m},1} = \Delta\theta/r_0$, respectively. Note the strong dependence of the interaction constant $\xi \sim r_0^3$ on the protein radius (for $r_0 \gg \zeta$); this is a consequence of both the rigidity of the protein (contributing $\sim r_0^2$) and the linear increase of the circumference with r_0. Dependence of ξ on the protein radius (r_0) is plotted in Fig. 12 for the characteristic decay length $\zeta = 0.9$ nm.

Note also that the last relation in Eq. (28), $\xi^* = 0$, follows from our assumption that the rigid protein has a sufficiently large radius that $\tilde{E}$ does not depend on the derivatives of $C(\omega)$ and $\theta(\omega)$ with respect to ω.

4.2. Advanced Model

In this subsection, we introduce more advanced theoretical model in order to estimate the constants H_{m} and ξ, where now the tilt deformation is explicitly taken into account [28]. In the model from Section 5.1, the tilt degree of freedom enters the model only through the characteristic decay length ζ.

In the model [28] we consider a lipid membrane that consists of two opposed monolayers, an external (E) and an internal (I) one. Both monolayers are described by a height profile, h_{E} and h_{I}, and by their local directors (unit vectors), $\mathbf{t}_{\mathrm{E}}$ and $\mathbf{t}_{\mathrm{I}}$, that describe the average orientation of the lipid chains (see Fig. 10).

The elastic free energy per unit area, $\hat{f}_{\mathrm{E}}$, of the external monolayer can be written up to quadratic order in h_{E} and $\mathbf{t}_{\mathrm{E}}$ as

$$\begin{aligned}\hat{f}_{\mathrm{E}} = {} & \frac{\kappa_{\mathrm{s}}}{2}\left(\nabla\cdot\mathbf{t}_{\mathrm{E}}\right)^2 + \frac{\kappa_{\mathrm{t}}}{2}\left(\mathbf{t}_{\mathrm{E}} - \nabla h_{\mathrm{E}}\right)^2 + \frac{B}{2}\left(h_{\mathrm{E}} - h\right)^2 + \frac{\kappa_{\mathrm{h}}}{2}\left(\Delta h_{\mathrm{E}}\right)^2 \\ & + \frac{K}{2}\left(\nabla \times \mathbf{t}_{\mathrm{E}}\right)^2 + \overline{\kappa}\det h_{\mathrm{E},ij}\end{aligned} \tag{29}$$

The first term in Eq. (29) characterizes the splay energy of the lipid chains with κ_{s} being the corresponding splay modulus. The second term accounts for the energy cost of tilting the director $\mathbf{t}_{\mathrm{E}}$ away from its orientation normal to the surface h_{E}; the

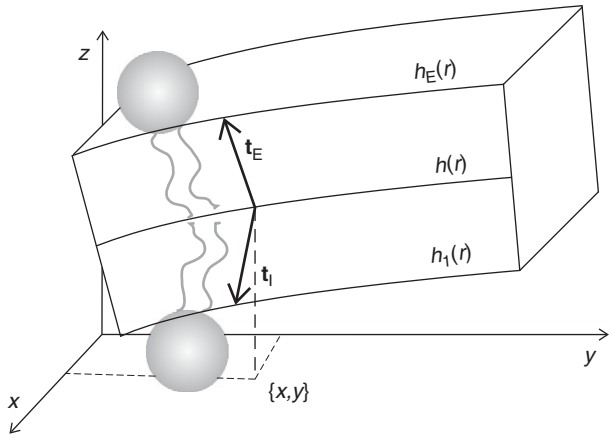

Figure 10 Illustration of a perturbed lipid bilayer with indicated local directors $\mathbf{t}_E$ and $\mathbf{t}_I$ and height profiles h_E and h_I of the external and internal leaflet, respectively. The average height of the bilayer is $h = (h_E + h_I)/2$. Two lipid molecules are shown schematically (adapted from [28]).

prefactor κ_t is the tilt modulus [42]. Thickness changes of the monolayer are accounted for by the third term where B is the compression modulus and h is the height of the reference surface with respect to which the compression/expansion of the monolayer is measured. It is reasonable to assume that for given membrane thickness $h_E - h_I$, the thickness of each monolayer is allowed to relax; this specifies $h = (h_E + h_I)/2$ to be the average height profile of the bilayer. The fourth term in Eq. (29) expresses the bare bending energy of the external monolayer with corresponding modulus κ_h. Note that this term is distinct from the splay energy; only for $\kappa_t \to \infty$ splay and bare bending refer to the same deformation. While the splay energy mainly accounts for the splay deformation of the lipid chains, the bending term originates predominantly in the headgroup region of the monolayer. For example, the electrostatic contribution to the bending modulus contributes entirely to κ_h. One might therefore refer to the modulus κ_h as the head group contribution to the bending stiffness. The last two terms in Eq. (29) describe the energetic contribution of a twist deformation of the chains (with corresponding modulus K) and of a saddle deformation of h_E (with the modulus $\overline{\kappa}$).

Starting from $\hat{f}_E$, we obtain the elastic free energy of the internal leaflet, $\hat{f}_I$, by replacing $h_E \to h_I$ and $\mathbf{t}_E \to -\mathbf{t}_I$ (the minus sign in the latter reflecting the opposite orientation of the two opposed monolayers). Hence,

$$\hat{f}_I = \frac{\kappa_s}{2}(\nabla \times \mathbf{t}_I)^2 + \frac{\kappa_t}{2}(\mathbf{t}_I + \nabla h_I)^2 + \frac{B}{2}(h_I - h)^2 + \frac{\kappa_h}{2}(\Delta h_I)^2 + \frac{K}{2}(\nabla \times \mathbf{t}_I)^2 + \overline{\kappa} \det h_{I,ij} \tag{30}$$

The elastic free energy of the lipid bilayer per unit area $\hat{f}_{\mathrm{bl}}$ is then

$$\hat{f}_{\mathrm{bl}} = \hat{f}_{\mathrm{E}} + \hat{f}_{\mathrm{I}}. \tag{31}$$

At this point it is convenient to switch to a new set of variables, namely to the average shape h and thickness dilation u, defined through $h_{\mathrm{E}} = h + u$ and $h_{\mathrm{I}} = h - u$ (see also Fig. 10). Similarly, we define the average director $\mathbf{t}$ and the difference director $\mathbf{d}$ via the relations $\mathbf{t}_{\mathrm{E}} = \mathbf{t} + \mathbf{d}$ and $\mathbf{t}_{\mathrm{I}} = \mathbf{t} - \mathbf{d}$. This allows us to express $\hat{f}_{\mathrm{bl}} = \hat{f}_{\mathrm{tu}} + \hat{f}_{\mathrm{dh}}$ as the sum of the two independent contributions [17]

$$\begin{aligned}\hat{f}_{\mathrm{tu}} = {} & \kappa_{\mathrm{s}}(\nabla \times \mathbf{t})^2 + \kappa_{\mathrm{t}}(\mathbf{t} - \nabla u)^2 + Bu^2 + \kappa_{\mathrm{h}}(\Delta u)^2 \\ & + K(\nabla \times \mathbf{t})^2 + 2\,\overline{\kappa}\,\det u_{ij}\end{aligned} \tag{32}$$

and

$$\begin{aligned}\hat{f}_{\mathrm{dh}} = {} & \kappa_{\mathrm{s}}(\nabla \times \mathbf{d})^2 + \kappa_{\mathrm{t}}(\mathbf{d} - \nabla h)^2 + \kappa_{\mathrm{h}}(\Delta h)^2 \\ & + K(\nabla \times \mathbf{d})^2 + 2\,\overline{\kappa}\,\det h_{ij}\end{aligned} \tag{33}$$

The two contributions can be treated separately. The first one depends on the tilt difference $\mathbf{t}$ and thickness dilation u which is relevant for proteins with up-down symmetry including the case of hydrophobic mismatch. The corresponding rigid protein-induced deformation is short-ranged and has been studied intensively in the past [39, 40]. In the present chapter, we focus our interest entirely on the second contribution (namely Eq. 33). In other words, we consider membrane deformations due to isotropic, cone-like rigid proteins with no hydrophobic mismatch (implying $\hat{f}_{\mathrm{tu}} = 0$). We thus seek to minimize the overall elastic free energy $F_{\mathrm{dh}} = \int\int \hat{f}_{\mathrm{dh}} \mathrm{d}a$ where $\mathrm{d}a = \mathrm{d}x\mathrm{d}y[1 + (\nabla h)^2]^{1/2}$ denotes the area element of the lipid bilayer. The corresponding Euler-Lagrange equations pertaining to F_{dh} are

$$\begin{aligned}\kappa_{\mathrm{t}}(\mathbf{d} - \nabla h) - \kappa_{\mathrm{s}}\nabla(\nabla \times \mathbf{d}) + K\nabla \times (\nabla \times \mathbf{d}) = 0 \\ \kappa_{\mathrm{h}}\nabla^4 h + \kappa_{\mathrm{t}}(\nabla \times \mathbf{d} - \Delta h) = 0\end{aligned} \tag{34}$$

To make the model tractable analytically, we assume a cylindrical symmetry around a rigid protein. In other words, we are in this subsection only interested in inclusions (i.e., membrane nanodomains) induced by isotropic membrane-embedded rigid proteins. Also, we adopt a cell model, that is, we assume that the inclusions are *homogeneously distributed* over a membrane segment of *prescribed* spherical curvature ($c_1 = c_2 = c$), defined at the mesoscopic level. The cell model starts from a hexagonal arrangement of spatially fixed cone-like inclusions of (average) radius r_0 [28] (see Fig. 11). The radius R of the unit cell (see Fig. 9) then defines the (uniform) area fraction $m = r_0^2/R^2$ of rigid proteins in the membrane segment. Our aim is to characterize—at the mesoscopic scale—the bending stiffness of a rigid

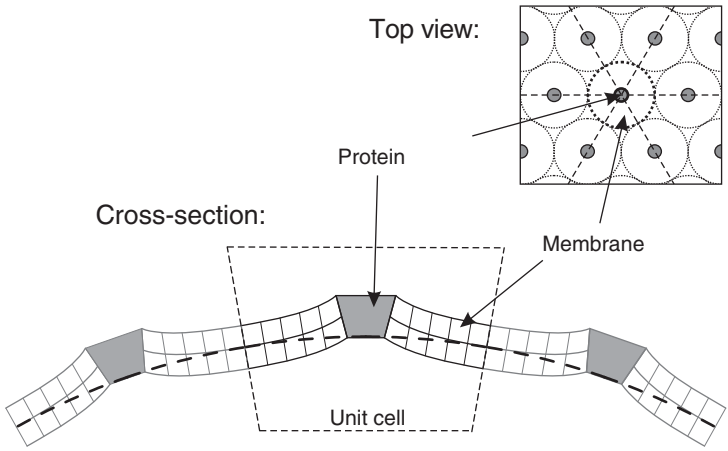

Figure 11 Top view: Schematic illustration of a hexagonal array of laterally fixed isotropic cone-like membrane-embedded rigid proteins (shaded circles). The unit cell around each protein is approximated by a circle. The membrane shape in the cross-section is also given. The shaded cones represent cross-sections through the inclusions (adapted from [28]).

protein-containing membrane patch with prescribed sphere-like membrane curvature. Hence, the membrane curvatures at the boundaries of each unit cell are fixed to be $c_1 = c_2 = c$, where c is the sphere-like (mesoscopic level) membrane curvature. The fact that the curvatures at the cell boundaries are all equal is a consequence of both the symmetry of the deformation and the isotropy of the protein. The local, microscopic, membrane shape perturbation within the unit cell is allowed to minimize the membrane free energy (see also Fig. 11).

Equation (34) can be solved analytically for cylindrical symmetry and the corresponding free energy F_{dh} can be calculated. This derivation is explained in detail elsewhere [28], here we discuss only the dependencies of the constants H_{m} and ξ [see Eq. (22)] on the parameters of the microscopic model.

In the model presented in Section 2, the single inclusion energy [Eq. (22)] induced by an isotropic rigid protein ($D_{\mathrm{m}} = 0$) in a spherical membrane curvature field ($H = c = \text{const.}$ and $D = 0$) simplifies to:

$$E = \mu_{\mathrm{m}} + \frac{\xi}{2}(H - H_{\mathrm{m}})^2, \tag{35}$$

where curvature c is defined at the mesoscopic level. In other words, the possible local microscopic curvature deformation around the rigid protein (Fig. 6B) is not shown directly in c, instead, it is hidden in the phenomenological parameters ξ and H_{m}.

By comparing Eq. (35) with the free energy F_{dh} from the model described above, we can obtain the relations [28]

$$H_{\mathrm{m}} \simeq \frac{(1+\kappa_{\mathrm{rel}})}{\kappa_{\mathrm{rel}}} c_0, \tag{36}$$

$$\xi \simeq \pi R^2 \kappa_0 \kappa_{\mathrm{rel}}. \tag{37}$$

Here κ_0 is the (local) bending stiffness of the (rigid protein-free) lipid bilayer, R is the radius of the cylindrically symmetric unit cell (Fig. 11), c_0 is the spontaneous curvature of the rigid protein-containing membrane, and κ_{rel} is the relative change of the bending stiffness κ due to the presence of the rigid proteins in the membrane bilayer; namely $\kappa_{\mathrm{rel}} = \kappa/\kappa_0 - 1$. The expressions for c_0 and κ_{rel} can be derived analytically [28]. In the compact form they can be written in terms of the relative cell size $\rho = (R/r_0)^2 - 1$ and the quantities

$$\eta^2 = \frac{\kappa_{\mathrm{h}}}{\kappa_{\mathrm{s}}}, \tag{38}$$

$$\tilde{\eta} = \frac{(1+\eta^2)}{\eta^2} = \left(\frac{\kappa_{\mathrm{s}}}{\kappa_{\mathrm{h}}}\right) + 1, \tag{39}$$

$$\overline{\alpha} = \frac{\overline{\kappa}}{[2(\kappa_{\mathrm{s}} + \kappa_{\mathrm{h}})]}, \tag{40}$$

$$\tilde{\zeta} = \left(\frac{\kappa_{\mathrm{t}}}{\kappa_{\mathrm{s}}} + \frac{\kappa_{\mathrm{t}}}{\kappa_{\mathrm{h}}}\right)^{-1/2} \tag{41}$$

and

$$P = \frac{2\tilde{\zeta}}{r_0} \frac{I_1(R/\tilde{\zeta})K_1(r_0/\tilde{\zeta}) - I_1(r_0/\tilde{\zeta})K_1(R/\tilde{\zeta})}{I_1(R/\tilde{\zeta})K_0(r_0/\tilde{\zeta}) + I_0(r_0/\tilde{\zeta})K_1(R/\tilde{\zeta})} \tag{42}$$

where I_n and K_n give the modified Bessel functions of the first and second kind, respectively. We find that

$$\frac{R^2 c_0}{\theta r_0} = \frac{-(1 - P\overline{\alpha}\tilde{\eta})(1+\rho)}{1 + \rho(1+\overline{\alpha}) + P\overline{\alpha}\eta^2\{1 - \tilde{\eta}^2[1 + \rho(1+\overline{\alpha})]\}} \tag{43}$$

and

$$\kappa_{\mathrm{rel}} = \frac{1}{1+\overline{\alpha}} \frac{1 - P\eta^2(1 + \overline{\alpha}\tilde{\eta}^2)}{\rho + P\eta^2(1 - \overline{\alpha}\tilde{\eta}^2\rho)} \tag{44}$$

Local stability condition implies $\kappa_0 > -\overline{\kappa}/2 > 0$ [12, 41] (where κ_0 and $\overline{\kappa}$ are local bending (splay) modulus and saddle-splay (Gaussian) modulus, respectively); therefore, $-0.5 < \overline{\alpha} < 0$. The estimated values of κ_t [42, 43] yield $\tilde{\zeta} \sim 0.2$nm.

The above expressions contain the microscopic membrane shape perturbations around a rigid protein through curvature deformation and through changes in lipid tilt (Fig. 6B). However, the model described in the present subsection can also be used for a biologically important case of restricted local shape perturbations (Fig. 6A). Relations for H_m and ξ [Eqs. (36) and (37)] remain the same, but the expression for the relative bending stiffness becomes

$$\kappa_{rel} = \frac{1}{1+\rho}\left[\frac{1}{P(1+\eta^2)(1+\overline{\alpha})} - 1\right], \tag{45}$$

where the function P is the same as in Eq. (42), with $\tilde{\zeta}$ now being replaced with $\tilde{\zeta}_c = \tilde{\zeta}(\kappa_h \to \infty)$:

$$\tilde{\zeta}_c = \left(\frac{\kappa_t}{\kappa_s}\right)^{-1/2}. \tag{46}$$

Relations (22), (36), and (37) are valid only as long as local deformations around the membrane-embedded neighboring rigid proteins do not overlap. Otherwise the interaction constant ξ [Eq. (22)] would depend on the area fraction of proteins ($m = r_0^2/R^2$) in the considered membrane patch. For the case of unconstrained local shape perturbations around the rigid proteins (Fig. 6B) the above relations are valid up to a certain value of the area fraction of the proteins. For most of the relevant cases, the actual area fraction of rigid proteins (m) is well below this value.

In the case of restricted local (microscopic) shape perturbations around the rigid protein (Fig. 6A), the decay of lipid (tilt) deformation around the protein is exponential (i.e., short-ranged). Therefore, the overlapping of the short-ranged lipid deformations around neighboring proteins becomes important only if the proteins are very close. Consequently, the interaction constants (ξ, ξ^*, H_m, and D_m) depend on the local density of the inclusions only for very large m.

For small values of m, we can expand the expression for ξ [Eq. (37)]. For unconstrained local membrane shape relaxation (Fig. 6B), we get

$$\xi = \frac{\pi r_0^2 \kappa_0}{1-\overline{\alpha}}\left[1 - \frac{2\eta^2\tilde{\zeta}(1+\overline{\alpha}\tilde{\eta}^2)}{r_0}\frac{K_1(r_0/\tilde{\zeta})}{K_0(r_0/\tilde{\zeta})}\right], \tag{47}$$

whereas the case of constrained local membrane shape relaxation (Fig. 6A) yields

$$\xi = \pi r_0^2 \kappa_0\left[\frac{r_0}{2\tilde{\zeta}_c(1+\eta^2)(1+\overline{\alpha})}\frac{K_0(r_0/\tilde{\zeta}_c)}{K_1(r_0/\tilde{\zeta}_c)} - 1\right]. \tag{48}$$

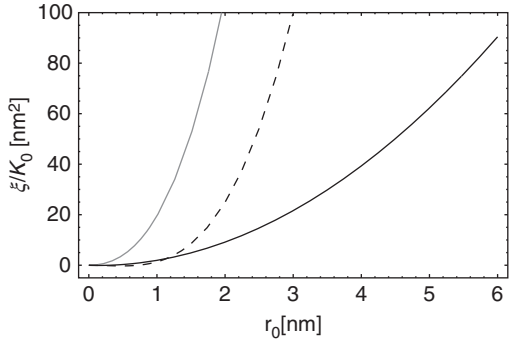

Figure 12 Interaction constant ξ [Eq. (22)] as a function of the average radius of the rigid protein (r_0) in the model of constrained local membrane microscopic shape perturbation (Fig. 6A) calculated from Eq. (28) for $\zeta = 0.9$ nm (gray full curve) and from Eq. (48) (dashed curve) for $\eta^2 = 1$, $\overline{\alpha} = -0.2$, and $\tilde{\zeta}_c = 0.2$ nm. The figure also shows the dependency of ξ on r_0 for unconstrained local membrane microscopic shape perturbation (Fig. 6B), as calculated from Eq. (47) for $\tilde{\zeta} = 0.2$ nm and same values of η^2 and $\overline{\alpha}$ (black solid curve).

It can be seen in Eqs. (47) and (48) that the interaction constant ξ adopts negative values for $r_0 < 2\tilde{\zeta}\eta^2(1+\overline{\alpha}\tilde{\eta}^2)K_1(r_0/\tilde{\zeta})/K_0(r_0/\tilde{\zeta})$ (unconstrained case) and $r_0 < 2\tilde{\zeta}_c(1+\eta^2)(1+\overline{\alpha})K_1(r_0/\tilde{\zeta}_c)/K_0(r_0/\tilde{\zeta}_c)$ (constrained case). Therefore, for large enough $\overline{\alpha}$ and $\tilde{\zeta}$ (or $\tilde{\zeta}_c$), and for small enough radius of the protein, rigid inclusions could locally soften the membrane [28]. This could not be predicted within the theory presented in Section 4.1, where the tilt degree of freedom is not explicitly taken into account and enters the model only through the characteristic decay length ζ.

In Fig. 12, the dependence of ξ on the average radius of the membrane-embedded rigid protein r_0 is shown for different presented models. The case of constrained local membrane shape perturbations (Fig. 6A) is shown in gray curve for the model from Section 4.1 and in dashed curve for the above described model [Eq. (48)]. The case of unconstrained local shape perturbations (Fig. 6A) is shown in black solid curve [see Eq. (47)].

5. Free Energy of Bilayer Membrane with Membrane-Embedded Inclusions

As already mentioned, the expression for the energy of membrane inclusion induced by single rigid membrane protein [Eq. (22)]:

$$E(\omega) = \frac{\xi}{2}(H - H_m)^2 + \frac{\xi + \xi^*}{4}(D^2 - 2DD_m\cos 2\omega + D_m^2), \qquad (49)$$

is mathematically equivalent to the expression for the energy of a single flexible membrane inclusion [see Eq. (4)], where

$$\xi = 2a_0(2K_1 + K_2), \quad \xi^* = -2a_0(2K_1 + 3K_2). \tag{50}$$

Therefore, in the following, only the expression (49) is used to describe the energy of a single inclusion.

It can be seen from Eq. (49) that the energy of a single inclusion attains a minimum when $\cos(2\omega) = 1$, while the single inclusion energy attains a maximum when $\cos(2\omega) = -1$. In the first case, the energy of a single inclusion is

$$E_{\min} = \frac{\xi}{2}(H - H_{\mathrm{m}})^2 + \frac{\xi + \xi^*}{4}(D^2 + D_{\mathrm{m}}^2) - \frac{\xi + \xi^*}{2}DD_{\mathrm{m}}, \tag{51}$$

whereas in the second case it is

$$E_{\max} = \frac{\xi}{2}(H - H_{\mathrm{m}})^2 + \frac{\xi + \xi^*}{4}(D^2 + D_{\mathrm{m}}^2) + \frac{\xi + \xi^*}{2}DD_{\mathrm{m}}. \tag{52}$$

The states $\omega = 0, \pi$ and $\omega = \pi/2, 3\pi/2$, respectively, are degenerate.

Since all orientations of the inclusion do not have the same energy, the partition function [44] of a single inclusion can be described within the four-state model (considering only orientations $\omega = 0, \pi/2, 3\pi/2, \pi$) as:

$$Q = 2\exp\left(\frac{-E_{\min}}{kT}\right) + 2\exp\left(\frac{-E_{\max}}{kT}\right). \tag{53}$$

The free energy of a single membrane inclusion can then be obtained by the expression

$$\begin{aligned} f_i = -kT\ln Q = \frac{\xi}{2}(H - H_{\mathrm{m}})^2 + \frac{\xi + \xi^*}{4}(D^2 + D_{\mathrm{m}}^2) \\ - kT\ln\left[\cosh\left((\xi + \xi^*)\frac{DD_{\mathrm{m}}}{2kT}\right)\right], \end{aligned} \tag{54}$$

where we omitted the constant terms that can be neglected for the case of constant total number of inclusions in the membrane.

In the following, we derive the free energy of a bilayer membrane with membrane-embedded inclusion. The excluded volume principle, that is, the finite volume of the membrane inclusions, is taken into account by applying the lattice statistics [44]. Therefore, the membrane is divided into small patches, which still contain a large number of molecules so that the methods of statistical physics can be used. The mesoscopic membrane curvature (see also Fig. 6) is taken to be constant over the patch. In a single patch, a lattice with M sites is imagined. There are

N inclusions in a given patch, each contributing the free energy f_i. The direct interactions between the inclusions are not taken into account. The canonical partition function of the patch is therefore:

$$Q^{\mathrm{P}} = \frac{Q^N M!}{N!(M-N)!}, \tag{55}$$

where the partition function of the single inclusion Q is defined by Eq. (53). The Helmholz free energy of the patch is $F^{\mathrm{P}} = -kT \ln Q^{\mathrm{P}}$:

$$F^{\mathrm{P}} \approx -NkT \ln Q + kTN \ln \frac{N}{M} + kT(M-N) \ln \left(1 - \frac{N}{M}\right), \tag{56}$$

where we applied the Stirling approximation $\ln x! \cong x \ln x - x$.

The free energy of all inclusions in the bilayer membrane can be obtained by summing the contributions of all patches in the membrane:

$$F_i = \int_A n f_{\mathrm{i}} m_0 \mathrm{d}A + kTm_0 \int_A (n \ln n + (1-n) \ln (1-n)) \mathrm{d}A, \tag{57}$$

where $n = N/M$ is the local membrane area fraction occupied by the membrane inclusions, $\mathrm{d}A$ is the membrane area element (area of the patch), and $m_0 = M/\mathrm{d}A = 1/a_0$, where a_0 is the area of the single inclusion.

The total free energy of the bilayer membrane with the embedded inclusions (F) can thus then be written as [1, 29]

$$\begin{aligned} \frac{F}{m_0 A} = (1-n) \int_A \frac{a_0 \kappa_0}{2} (2H)^2 \mathrm{d}a + n \int_A f_i \mathrm{d}a \\ + kT \int_A (n \ln n + (1-n) \ln (1-n)) \mathrm{d}a, \end{aligned} \tag{58}$$

where A is the membrane area, $\mathrm{d}a = \mathrm{d}A/A$, and κ_0 is the (local) bending constant of the bilayer membrane. The first term accounts for the bending energy of the lipid bilayer, while the last term accounts for the configurational entropy of the inclusions [1, 29].

6. Conclusions

Theoretical approaches to study the coupling of non-homogeneous lateral distribution of membrane inclusions and membrane shapes [10, 29] were described for flexible membrane inclusions and for inclusions induced by rigid membrane proteins [1, 17]. As it is shown in this work, both cases yield a mathematically

equivalent result for the energy of a single membrane inclusion [see Eqs. (4) and (22)]. In the first case of flexible inclusions, the phenomenological constants K_1 and K_2 originate in the deformation of the small membrane complex (nanodomain) composed of lipids and proteins (Fig. 1A) and depend on the elastic and geometric properties of this complex (membrane nanodomain); while in the second case (where inclusion is induced by the rigid globular protein), the globular proteins are treated as rigid bodies (Fig. 1B) and the whole contribution to the interaction constants ξ and ξ^* [Eq. (22)] originate in the deformation of the surrounding lipid molecules and the geometry of the rigid protein. The value of the interaction constant ξ grows with the average radius of the rigid protein (r_0) (Fig. 12).

In biological membranes, the majority of the membrane rigid proteins are laterally distributed over the whole membrane area. In addition, the number of the membrane proteins (N) is very large. For such systems, the case of *constrained* microscopic perturbation of the membrane shape around the intercalated rigid protein (Fig. 6A) seems to be biologically more relevant than the case of *unconstrained* microscopic perturbation of the membrane shape around the intercalated rigid protein (Fig. 6B).

As for example in erythrocytes, the budding takes place over the whole cell membrane surface (although it is located predominately at the top of membrane spicules) [1, 12]. Because of that, local microscopic membrane shape perturbations around the membrane-embedded proteins are strongly restricted (see Eq. 18). As a consequence, the lipid deformation around the membrane-embedded proteins is predominantly a consequence of the change of tilt of lipid molecules around the proteins (Fig. 6A), and not of the microscopic membrane shape perturbation (Fig. 6B).

Coupling between non-homogeneous lateral distribution of membrane-embedded rigid proteins and specific membrane shapes may be an important mechanism of generation and stabilization of highly curved membrane structures. Therefore, the theoretical models of membrane inclusions described in this chapter provide a tool to study processes in membranes that involve membrane regions with high curvatures, like spherical buds [1], membrane necks [45, 46], or thin tubular membrane protrusions [12, 47].

ACKNOWLEDGMENTS

The authors appreciate the collaboration with S. May and H. Hägerstrand and are grateful to Blaž Babnik for technical assistance.

REFERENCES

[1] H. Hägerstrand, L. Mrowczynska, U. Salzer, R. Prohaska, K.A. Michelsen, V. Kralj-Iglič, A. Iglič, Curvature dependent lateral distribution of raft markers in the human erythrocyte membrane, Mol. Membr. Biol. 23 (2006) 277–288.
[2] H. Gruler, Chemoelastic effect of membranes, Z. Naturforsch. 30c (1975) 608–614.

[3] W. Helfrich, J. Prost, Intrinsic bending force in anisotropic membranes made of chiral molecules, Phys. Rev. A 38 (1988) 3065–3068.
[4] R. Oda, I. Huc, M. Schmutz, S.J. Candau, F.C. MacKintosh, Tuning bilayer twist using chiral counterions, Nature 399 (1999) 566–569.
[5] A. Iglič, B. Babnik, U. Gimsa, V. Kralj-Iglič, On the role of membrane anisotropy in the beading transition of undulated tubular membrane structures, J. Phys. A: Math Gen. 38 (2005) 8527–8536.
[6] A. Iglič, M. Tzaphlidou, M. Remškar, B. Babnik, M. Daniel, V. Kralj-Iglič, Stable shapes of thin anisotropic nano-strips, Fullerenes Nanotubes Carbon Nanostruct. 13 (2005) 183–192.
[7] L.D. Landau, E.M. Lifshitz, Theory of Elasticity (3rd ed.), Butterworth-Heinemann, Oxford, 1997.
[8] A. Iglič, T. Slivnik, V. Kralj-Iglič, Elastic properties of biological membranes influenced by attached proteins, J. Biomech. 40 (2007) 2492–2500.
[9] D.V. Widder, Advanced Calculus, Prentice-Hall, Inc., New York, 1947.
[10] V. Kralj-Iglič, S. Svetina, B. Zeks, Shapes of bilayer vesicles with membrane embedded molecules, Eur. Biophys. J. 24 (1996) 311–321.
[11] V. Kralj-Iglič, V. Heinrich, S. Svetina, B. Žekš, Free energy of closed membrane with anisotropic inclusions, Eur. Phys. J. B 10 (1999) 5–8.
[12] V. Kralj-Iglič, H. Hägerstrand, P. Veranič, K. Jezernik, A. Iglič, Amphiphile-induced tubular budding of the bilayer membrane, Eur. Biophys. J. 34 (2005) 1066–1070.
[13] M. Fosnarič, K. Bohinc, D.R. Gauger, A. Iglič, V. Kralj-Iglič, S. May, The influence of anisotropic membrane inclusions on curvature elastic properties of lipid membranes, J. Chem. Inf. Mod. 45 (2005) 1652–1661.
[14] S. Marčelja, Chain ordering in liquid crystal II. Structure of bilayer membranes, Biochim. Biophys. Acta 367 (1974) 165–176.
[15] S. Marčelja, Lipid-mediated protein interaction in membranes, Biochim. Biophys. Acta 455 (1976) 1–7.
[16] W. Helfrich, Elastic properties of lipid bilayers: Theory and possible experiments, Z. Naturforsch. 28 (1973) 693–703.
[17] J.B. Fournier, Microscopic membrane elasticity and interactions among membrane inclusions: Interplay between the shape, dilation, tilt and tilt-difference modes, Eur. Phys. J. B 11 (1999) 261–272.
[18] M. Rappolt, A. Hickel, F. Bringezu, K. Lohner, Mechanism of the lamellar/inverse hexagonal phase transition examined by high resolution X-ray diffraction, Biophys. J. 84 (2003) 3111–3122.
[19] S. May, A. Ben-Shaul, Molecular theory of lipid-protein interaction and the L_α–H_π transition, Biophys. J. 76 (1999) 751–767.
[20] T.C. Lubensky, F.C. MacKintosh, Theory of ''ripple'' phases of lipid bilayers, Phys. Rev. Lett. 71 (1993) 1565–1568.
[21] J.B. Fournier, Coupling between membrane tilt-difference and dilation: A new ''ripple'' instability and multiple crystalline inclusions phases, Europhys. Lett. 43 (1998) 725–730.
[22] U. Seifert, J. Shillcock, P. Nelson, Role of bilayer tilt difference in equilibrium membrane shapes, Phys. Rev. Lett. 77 (1996) 5237–5240.
[23] P.G. Dommersnes, J.B. Fournier, N-body study of anisotropic membrane inclusions: membrane mediated interactions and ordered aggregation, Eur. Phys. J. B 12 (1999) 9–12.
[24] P.G. Dommersnes, J.B. Fournier, The many-body problem for anisotropic membrane inclusions and the self-assembly of ''Saddle'' defects into an ''Egg Carton'', Biophys. J. 83 (2002) 2898–2905.
[25] W. Helfrich, Blocked lipid exchange in bilayers and its possible influence on the shape of vesicles, Z. Naturforsch 29c (1974) 510–515.
[26] E.A. Evans, R. Skalak, Mechanics and Thermodynamics of Biomembranes, CRC Press, Boca Raton, Florida, 1980.
[27] W.C. Hwang, R.E. Waugh, Energy of dissociation of lipid bilayers from the membrane skeleton of red cells, Biophys. J. 72 (1997) 2669–2678.
[28] M. Fošnarič, A. Iglič, S. May, Influence of rigid inclusions on the bending elasticity of a lipid membrane, Phys. Rev. E 174 (2006) 051503/1–051503/12.
[29] V.S. Markin, Lateral organization of membranes and cell shapes, Biophys. J. 36 (1981) 1–19.

[30] U. Seifert, Configurations of fluid membranes and vesicles, Adv. In Phys. 46 (1997) 13–137.
[31] M. Laradji, P.B.S. Kumar, Dynamics of domain growth in self-assembled fluid vesicles, Phys. Rev. Lett. 93 (2004) 198105/1–4.
[32] J.M. Allain, M. Ben Amar, Biphasic vesicle: Instability induced by adsorption of proteins, Physica A 337 (2004) 531–545.
[33] U. Seifert, Curvature-induced lateral phase segregation in two-component vesicles, Phys. Rev. Lett. 70 (1993) 1335–1338.
[34] S. Leibler, Curvature instability in membranes, J. Phys. (France) 47 (1986) 507–516.
[35] L.B. Fournier, Nontopological saddle-splay and curvature instabilities from anisotropic membrane inclusions, Phys. Rev. Lett. 76 (1996) 4436–4439.
[36] B. Božič, V. Kralj-Iglič, S. Svetina, Coupling between vesicle shape and lateral distribution of mobile membrane inclusions, Phys. Rev. E 73 (2006) 041915/1–11.
[37] S. May, Membrane perturbations induced by integral proteins: Role of conformational restrictions of the lipid chains, Langmuir 18 (2002) 6356–6364.
[38] N. Dan, S.A. Safran, Effect of lipid characteristics on the structure of transmembrane proteins, Biophys. J. 75 (1998) 1410–1414.
[39] N. Dan, P. Pincus, S.A. Safran, Membrane-induced interactions between inclusions, Langmuir 9 (1993) 2768–2771.
[40] C. Nielsen, M. Goulian, O.S. Andersen, Energetics of inclusion-induced bilayer deformations, Biophys. J. 74 (1998) 1966–1983.
[41] A. Ben-Shaul, Molecular theory of chain packing, elasticity and lipid-protein interactions in lipid bilayers, in: R. Lipowsky, E. Sackmann (Eds.), Structure and Dynamics of Membranes, Elsevier, Amsterdam, 1995, p. 382.
[42] W. Helfrich, Elastic properties of lipid bilayers: Theory and possible experiments, Z. Naturforsch. 28c (1973) 693–703.
[43] S. May, Y. Kozlovsky, A. Ben-Shaul, M.M. Kozlov, Tilt modulus of lipid monolayer, Eur. Phys. J. E 14 (2004) 299–308.
[44] T.L. Hill, An Introduction to Statistical Thermodynamics, General Publishing Company, Toronto, 1986, pp. 209–211.
[45] A. Iglič, B. Babnik, K. Bohinc, M. Fošnarič, H. Hägerstrand, V. Kralj-Iglič, On the role of anisotropy of membrane constituents in formation of a membrane neck during budding of a multicomponent membrane, J. Biomech. 40 (2007) 579–585.
[46] V. Kralj-Iglič, P. Veranič, Curvature-induced sorting of bilayer membrane constituents and formation of membrane rafts, in: A. Leitmannova Liu (Ed.), Advances in Planar Lipid Bilayers and Their Liposomes, Elsevier, Amsterdam, London, 2007, pp. 129–149.
[47] A. Iglič, H. Hägerstrand, P. Veranič, A. Plemenitaš, V. Kralj-Iglič, Curvature induced accumulation of anisotropic membrane components and raft formation in cylindrical membrane protrusions, J. Theor. Biol. 240 (2006) 368–373.